



## Solution-processed ZnO-chemically converted graphene gas sensor

Tran Viet Cuong<sup>a</sup>, Viet Hung Pham<sup>a</sup>, Jin Suk Chung<sup>a</sup>, Eun Woo Shin<sup>a</sup>, Dae Hwang Yoo<sup>b</sup>, Sung Hong Hahn<sup>b</sup>, Jeung Soo Huh<sup>c</sup>, Gi Hong Rue<sup>c</sup>, Eui Jung Kim<sup>a,\*</sup>, Seung Hyun Hur<sup>a,\*</sup>, Paul A. Kohl<sup>d</sup>

<sup>a</sup> Department of Chemical Engineering, University of Ulsan, Ulsan 680-749, South Korea

<sup>b</sup> Department of Physics, University of Ulsan, Ulsan 680-749, South Korea

<sup>c</sup> School of Electrical Engineering and Computer Science, Kyungpook National University, Daegu 702-701, South Korea

<sup>d</sup> School of Chemical and Biomolecular Engineering, Georgia Institute of Technology, Atlanta, Georgia 30332-0100, USA

### ARTICLE INFO

#### Article history:

Received 4 May 2010

Accepted 5 August 2010

Available online 10 August 2010

#### Keywords:

Sensors

Solution synthesis

Graphene films

ZnO nanorods

### ABSTRACT

We report a solution-processed gas sensor based on vertically aligned ZnO nanorods (NRs) on a chemically converted graphene (CCG) film. The prepared sensor device effectively detected 2 ppm of H<sub>2</sub>S in oxygen at room temperature. A high sensitivity of the gas sensor resulted from the growth of highly dense vertical ZnO NRs on the CCG film with numerous tiny white dots on its surface, which may provide a sufficient number of sites for the nucleation and growth of the ZnO NRs. The adsorption of oxygen on the surface of the ZnO NRs was found to be crucial for obtaining an excellent gas sensing performance of the ZnO NRs-CCG sensor.

© 2010 Elsevier B.V. All rights reserved.

## 1. Introduction

In the past decade, one-dimensional (1-D) nanostructures such as carbon nanotubes, ZnO nanowires (NWs) or nanorods (NRs) have attracted much attention in sensor device applications [1]. Recently, two-dimensional (2-D) graphene has emerged as a high potential material and increasingly attracted attention owing to its fascinating physical properties including quantum electronic transport, extremely high mobility, high elasticity, and electromechanical modulation [2]. Future studies require a building block of multifunctional materials as well as structures, because it enables us to exploit versatile and tailor-made properties with performances far beyond those of the individual materials and also opens the door to a wide range of possible applications. In this regard, attempts have been made to integrate 1-D ZnO NRs with 2-D graphene to synthesize the novel material structure for investigating its optoelectrical properties and its application in gas sensor devices. In this work, we present a straightforward solution-based method to prepare a gas sensor device from ZnO NRs vertically grown on a chemically converted graphene (CCG) thin film that increases the density of vertically aligned ZnO NRs with preferred orientation along the (002) plane.

## 2. Experimental

A ZnO-graphene gas sensor was fabricated by a simple solution-based process that consists of two main steps: synthesis of CCG film and direct growth of ZnO NRs on it. The preparation of the CCG film is described in detail elsewhere [3]. To prepare a ZnO seed layer, the CCG film was wetted with an ethanolic solution of 5 mM zinc acetate dehydrate (98%, Aldrich), rinsed with ethanol after 10 s, and dried by blowing with a stream of argon. This coating step was repeated five times. The CCG film coated with a thin layer of zinc acetate crystallites was heated to 350 °C in air for 30 min to form the ZnO seed layer. Finally, the ZnO NRs were directly grown by placing the substrate on a stainless steel holder in a 100 mL aqueous solution of 16 mM zinc nitrate hexahydrate and 25 mM methanamine, and heating the solution at 90 °C in an oven for 4 h. The substrates covered with the ZnO NRs were rinsed with water and dried in an argon stream. The surface morphology, crystal phase and crystallinity of the samples were investigated by scanning electron microscopy (SEM), atomic force microscopy (AFM), Raman spectroscopy (Witec alpha 300SR) and high resolution X-ray diffraction (HRXRD, Bruker D8 Advance), respectively.

The ZnO NRs-CCG sensor was inserted on a panel and then placed in a sealed chamber with heating facility. N<sub>2</sub> and O<sub>2</sub> were used as carrier gases and H<sub>2</sub>S as a test gas. Prior to H<sub>2</sub>S detection, the sensor was soaked in N<sub>2</sub> or O<sub>2</sub> until the sensor resistance reached a stationary value. The gas flow rate was controlled with a mass flow controller. The change of the sensor resistance due to H<sub>2</sub>S adsorption was

\* Corresponding authors. Tel.: +82 52 259 2832; fax: +82 52 259 1689.

E-mail addresses: [ejkim@ulsan.ac.kr](mailto:ejkim@ulsan.ac.kr) (E.J. Kim), [shhur@ulsan.ac.kr](mailto:shhur@ulsan.ac.kr) (S.H. Hur).

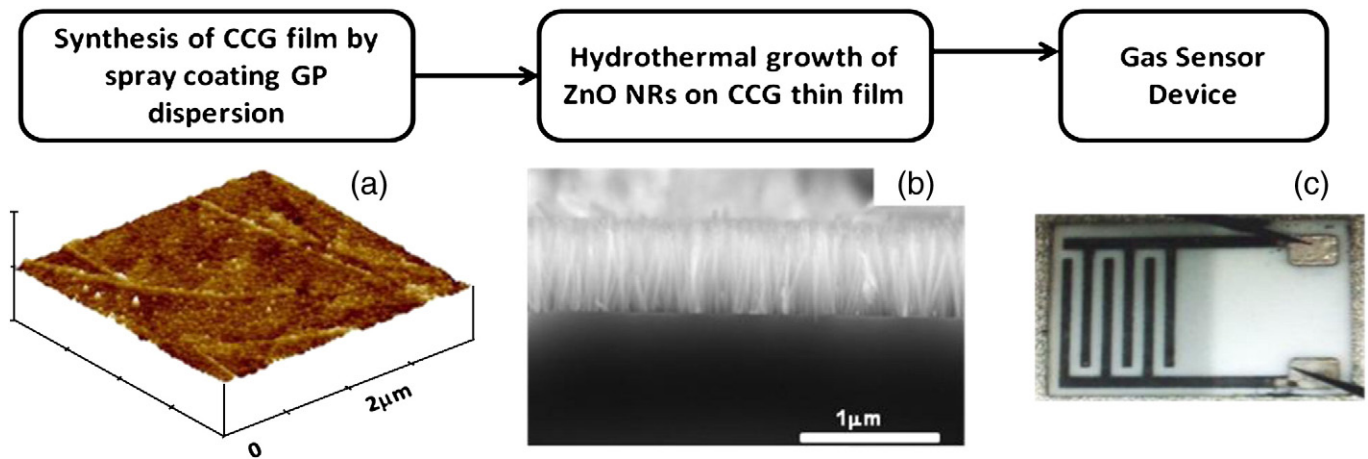


Fig. 1. (a) 3-dimensional AFM surface morphology of the CCG thin film with dots, (b) SEM image of ZnO NRs directly grown on the CCG film, and (c) gas sensor device.

monitored, analyzed and stored by a computer with DAQ (data acquisition board) and Lab-VIEW software.

### 3. Results and discussion

Fig. 1 depicts the fabrication process of a ZnO NRs-CCG gas sensor that consists of two main steps: synthesis of CCG film and direct growth of ZnO NRs on this film. The surface morphology of the produced CCG film with small white dots which were formed during spray-coating of graphene oxide (GO)-hydrazine dispersion at a low temperature was clearly observed in Fig. 1(a). At a low temperature, the reduction rate is slow and thus the GO sheets are reduced after deposition onto the substrate. Consequently the by-products of reduction, such as  $H_2O$ ,  $NO_2$ , and  $N_2$  are trapped in the CCG sheets, resulting in the formation of small white dots. The cross-sectional SEM image of the ZnO NRs grown on the CCG film is exhibited in Fig. 1(b). The ZnO NRs were found to be vertically grown on the CCG film and the ZnO NRs had typically a length of 0.5–2  $\mu m$  with a diameter of around 100 nm. Fig. 1(c) shows a ceramic plate of the ZnO NRs-CCG

sensor employed in our study. Pt alloy electrodes were coated with an interdigit structure on one side and heater patterns of  $RuO_2$  were pasted on the other side by a screen printing method.

To explore the effect of dot on the nanorod growth, ZnO NRs were grown on the CCG film with and without dots under identical growth condition. The dot may form a step edge in the CCG layer. The nucleation and growth of the ZnO are more favourable along the step edge [4]. In addition, the dots may serve as nucleation centers for nanorod growth. Consequently, ZnO NRs grown on the CCG layer with dots (Fig. 2(a)) had a larger diameter size compared to those grown on the CCG layer without dots (Fig. 2(b)). In Fig. 2(c), the HRXRD spectra of ZnO NRs on the CCG layer with dots possessed a sole strong peak of the (002) plane implying that the ZnO NRs were grown along the c-axis. On the other hand, several peaks were observed for ZnO NRs grown on the CCG layer without dots (Fig. 2(d)). The HRXRD results are well consistent with the SEM images.

Fig. 3(a) exhibits the PL spectra of the sample. Generally, a UV emission peak centered around 380 nm corresponds to the near band edge emission and a yellow emission broadband is related to the

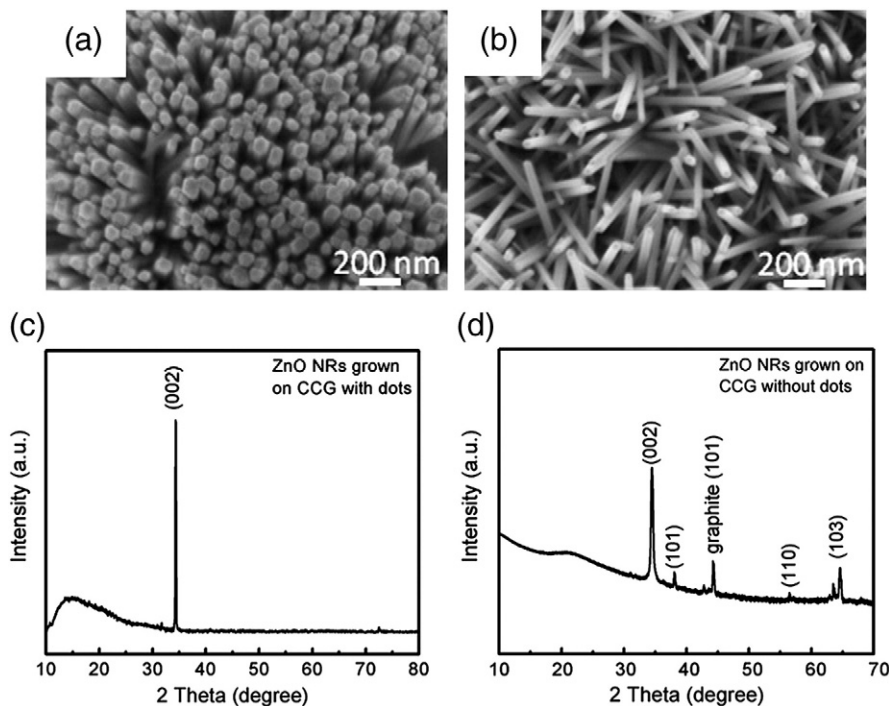
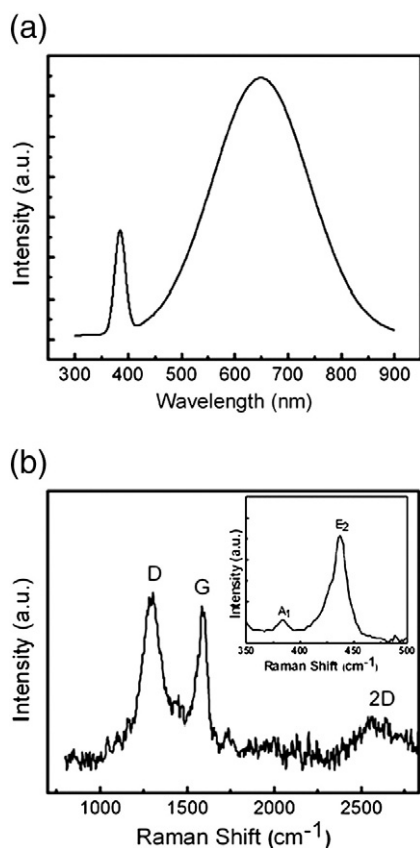


Fig. 2. SEM images and HRXRD spectra of ZnO NRs on (a, c) the CCG film with dots and (b, d) without dots.



**Fig. 3.** (a) Photoluminescence and (b) Raman spectra of ZnO NRs directly grown on the CCG film with dots.

intrinsic defects in the sample. Particularly, broad and intense yellow emission may arise from two emission mechanisms: single ionized oxygen vacancy in ZnO NRs and the recombination of electron-hole pairs localized within small  $sp^2$  carbon clusters embedded within a  $sp^3$  matrix in the CCG film [5–7]. Fig. 3(b) shows the Raman spectra of ZnO NRs grown on the CCG film. Two prominent peaks such as D ( $1340\text{ cm}^{-1}$ ) and G ( $1584\text{ cm}^{-1}$ ) for a typical CCG film are clearly observed in the Raman spectra. A very weak 2D band at  $\sim 2700\text{ cm}^{-1}$  and a noticeably high intensity of the D peak imply that the CCG film has considerable defects. In addition, the inset of Fig. 2(b) shows that a strong peak at  $438\text{ cm}^{-1}$  is attributed to ZnO nonpolar optical phonons with the  $E_2$  mode, while a weak peak at  $383\text{ cm}^{-1}$  corresponds to  $A_1$  symmetry with the TO mode.

Fig. 4 shows typical sensitivity curves of ZnO NRs-CCG sensors under different test conditions. The sensitivity of the sensor is defined as  $[(R_g - R_0)/R_0 \times 100]$ , where  $R_0$  and  $R_g$  are the sensor resistance before and after  $H_2S$  exposure, respectively. In Fig. 4(a), the ZnO NRs-CCG sensor was initially exposed to oxygen at room temperature (RT). Oxygen molecules are adsorbed on the surface of the ZnO NRs and form oxygen ionic species by capturing electrons from the conduction band. As a result, the sensor possessed a high resistance in the oxygen environment. When  $H_2S$  gas was introduced,  $H_2S$  would react with the surface oxygen species, which decreased the surface concentration of oxygen ions and increased the electron concentration. This led to a decrease in the resistance of the ZnO NRs-CCG sensor. A sensor device based on the CCG film without ZnO NRs was also made and tested under identical conditions. In this case, the resistance increased when the CCG sensor was exposed to  $H_2S$  in an oxygen environment at RT. Oxygen functionalities such as epoxide and carboxyl groups existing in CCG are electron-withdrawing groups and promote some holes into the conduction band. The introduction of reductive agent  $H_2S$  actually caused depletion of holes from the conduction band and

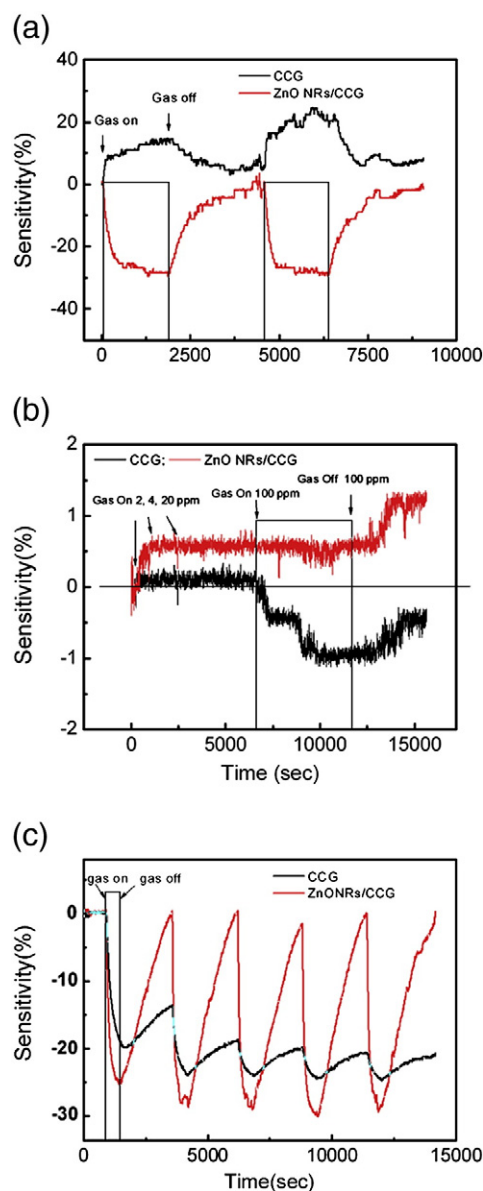


**Fig. 4.** The sensitivity of ZnO NRs-CCG sensors to  $H_2S$  gas in (a) oxygen at RT and (b) nitrogen at RT, and (c) nitrogen at  $270\text{ }^\circ\text{C}$ .

hence raised the resistance [2]. We observed that the sensitivity was significantly lowered under a nitrogen environment at RT even with a high flow rate of  $H_2S$  as shown in Fig. 4(b). It means that oxygen molecules play a role in sensing  $H_2S$  gas. Interestingly, the sensitivity under nitrogen environment was markedly improved at  $270\text{ }^\circ\text{C}$ , as shown in Fig. 4(c). A possible explanation is that the thermal energy facilitates evaporation of by-products captured within the CCG underlayer. Moreover, the reduction of oxygen-containing groups could be initiated at  $250\text{ }^\circ\text{C}$  [8]. This led to a reduction in the electrical resistance of the CCG film. Oxygen molecules produced in thermal reduction and evaporation processes may be adsorbed on the surface of the ZnO NRs, resulting in the improved sensitivity of ZnO even under a nitrogen environment.

#### 4. Conclusions

SEM and XRD results demonstrated that ZnO NRs grown on the CCG film with dots were well-aligned in the  $c$ -axis orientation. Dots formed on the surface of the CCG underlayer helped increase the density and the size of ZnO NRs by providing a sufficient number

of sites for nucleation and growth. The prepared ZnO-CCG gas sensor device was able to detect 2 ppm of H<sub>2</sub>S in oxygen at room temperature. Our results suggested that the CCG film releases oxygen molecules during thermal reduction and evaporation of the by-product process, which are adsorbed on the surface of ZnO NRs, thereby improving gas sensitivity. There are still open questions about the release of oxygen from the reduced CCG film to maintain a high sensitivity of the device under a nitrogen environment for an extended period. We are currently investigating this issue in an effort to further improve the device performance for effective sensor applications.

## References

- [1] Liao L, Lu HB, Li JC, He H, Wang DF, Fu DJ, et al. *J Phys Chem C* 2007;111:1900–3.
- [2] Fowler JD, Allen MJ, Tung VC, Yang Y, Kaner RB, Weiller BH. *ACS Nano* 2009;3:301–6.
- [3] Pham VH, Cuong TV, Hur SH, Shin EW, Kim JS, Chung JS, et al. *Carbon* 2010;48:1945–51.
- [4] Kim YJ, Lee JH, Yi GC. *Appl Phys Lett* 2009;95:213101–3.
- [5] Hu JQ, Bando Y. *Appl Phys Lett* 2003;82:1401–3.
- [6] Eda BG, Lin YY, Mattevi C, Yamaguchi H, Chen HA, Chen IS, et al. *Adv Mater* 2010;22:505–9.
- [7] Cuong TV, Pham VH, Tran QT, Hahn SH, Chung JS, Shin EW, et al. *Mater Lett* 2010;64:399–401.
- [8] Akhavan O. *Carbon* 2010;48:509–19.